Çukurova Üniversitesi
Mühendislik Fakültesi Dergisi
Çukurova University
Journal of the Faculty of Engineering
ISSN: 2757-9255 CİLT/VOLUME: 41 SAYI/ISSUE: 1 MART/MARCH 2026

Binary and Multi-Class Chest X-Ray Classification for COVID-19 and Pneumonia Detection

Çiğdem Gülüzar ALTINTOP [1,a], **Tuğba ŞENTÜRK** [2,b], **Fatma LATİFOĞLU** [1,3,c]

[1]*Erciyes University, Engineering Faculty, Biomedical Engineering Department, Kayseri, Türkiye*
[2]*İnönü University, Engineering Faculty, Biomedical Engineering Department, Malatya, Türkiye*
[3]*Neural Informatics Technologies Inc., Erciyes Technopark, Kayseri, Türkiye*

[a]***ORCID**: 0000-0001-8632-3385; [b]**ORCID**: 0000-0002-1323-5752; [c]**ORCID**: 0000-0003-2018-9616*

Article Info
Received : 24.07.2025
Accepted : 01.12.2025
DOI: 10.21605/cukurovaumfd.1749930

Corresponding Author
Fatma LATİFOĞLU
flatifoglu@erciyes.edu.tr

Keywords
COVID-19
Coronavirus
Pneumonia
X-ray imaging
Deep learning

***How to cite:** ALTINTOP, Ç.G., ŞENTÜRK, T., LATİFOĞLU, F., (2026). Binary and Multi-Class Chest X-Ray Classification for COVID-19 and Pneumonia Detection. Cukurova University, Journal of the Faculty of Engineering, 41(1), 29-43.*

ABSTRACT

The Lung disorders, encompassing conditions such as pneumonia and COVID-19, represent significant challenges to global health, impacting millions annually. This study investigates the application of advanced deep learning architectures, specifically AlexNet and SqueezeNet, for the automated classification of chest X-ray (CXR) images from patients diagnosed with pneumonia, COVID-19, and healthy individuals. We achieved an impressive accuracy of 99.85% in binary classification tasks with SqueezeNet and 97.72% for multi-class classification. The results indicate that SqueezeNet outperformed AlexNet in sensitivity, specificity, and accuracy, particularly in distinguishing between COVID-19 and pneumonia. This highlights SqueezeNet's computational efficiency and effectiveness in rapid diagnostic applications. Our findings underscore the importance of timely diagnosis in improving outcomes, especially in resource-limited settings. The use of computer-aided diagnosis (CAD) technologies can aid in early detection and appropriate treatment. Future work will explore deep neural network models on heterogeneous and unbalanced datasets and apply these methods to CT images to enhance generalizability.

COVID-19 ve Zatürre Tespiti için İkili ve Çok Sınıflı Göğüs Röntgeni Sınıflandırması

Makale Bilgileri
Geliş : 24.07.2025
Kabul : 01.12.2025
DOI: 10.21605/cukurovaumfd.1749930

Sorumlu Yazar
Fatma LATİFOĞLU
flatifoglu@erciyes.edu.tr

Anahtar Kelimeler
COVID-19
Koronavirüs
Zatürre
Röntgen görüntüleme
Derin öğrenme

***Atıf şekli:** ALTINTOP, Ç.G., ŞENTÜRK, T., LATİFOĞLU, F., (2026). COVID-19 ve Zatürre Tespiti için İkili ve Çok Sınıflı Göğüs Röntgeni Sınıflandırması. Çukurova Üniversitesi, Mühendislik Fakültesi Dergisi, 41(1), 29-43.*

ÖZ

Zatürre ve COVID-19 gibi hastalıkları içeren akciğer bozuklukları, her yıl milyonlarca insanı etkileyerek küresel sağlık için önemli zorluklar oluşturmaktadır. Bu çalışma, zatürre, COVID-19 ve sağlıklı bireylerden elde edilen göğüs röntgeni görüntülerinin otomatik sınıflandırılması için özellikle AlexNet ve SqueezeNet gibi gelişmiş derin öğrenme mimarilerinin uygulanmasını incelemektedir. SqueezeNet ile ikili sınıflandırma görevlerinde %99.85 gibi etkileyici bir doğruluk, çok sınıflı sınıflandırma için ise %97.72 doğruluk elde edilmiştir. Sonuçlar, özellikle COVID-19 ile zatürreyi ayırt etmede, SqueezeNet'in duyarlılık, özgüllük ve doğruluk açısından AlexNet'ten daha iyi performans gösterdiğini ortaya koymaktadır. Bu durum, SqueezeNet'in hızlı tanı uygulamalarındaki hesaplama verimliliğini ve etkinliğini vurgulamaktadır. Bulgularımız, özellikle kaynakların kısıtlı olduğu ortamlarda, zamanında tanının hasta sonuçlarını iyileştirmedeki önemini ortaya koymaktadır. Bilgisayar destekli tanı (CAD) teknolojilerinin erken tespit ve uygun tedaviye katkı sağlayabileceği değerlendirilmektedir. Gelecek çalışmalar, heterojen ve dengesiz veri kümeleri üzerinde derin sinir ağı modellerini araştıracak ve bu yöntemleri BT görüntülerine uygulayarak genellenebilirliği artırmayı hedefleyecektir.

1. INTRODUCTION

Lung disorders include a wide range of problems that affect the lungs and respiratory system, resulting in reduced lung function and breathing. A variety of viral, bacterial or fungal illnesses can cause them. Environmental variables have been related to lung disorders including asthma, mesothelioma, and cancer. They also impact respiratory health, including chronic obstructive pulmonary disease (COPD) and infections like tuberculosis, pneumonia and influenza [1,2]. Pneumonia affects one or both lungs and causes inflammation of the lung parenchyma, which is the part of the lung tissue responsible for gas exchange, including the pulmonary alveoli. Inflammation causes the lung's alveoli to fill up with mucus or liquid, leading in symptoms such as shortness of breath, cough, chest discomfort, fever, and so on. Coronaviruses, commonly known as Severe Acute Respiratory Syndrome Coronavirus (SARS-CoV-2), are a group of viruses that may damage the whole human population [3]. Coronavirus illness, frequently referred to as 'COVID-19', was first found in December 2019. Pneumonia remains a serious global health challenge, contributing to high death rates worldwide. It is a leading cause of mortality among children under five years old in developing nations and among the elderly (over 65 years old) in developed countries [4,5]. The SARS-CoV-2 virus has further exacerbated this situation, causing widespread disruption. Globally, up to the present day, there have been over 702 million confirmed cases of COVID-19, resulting in approximately 6.9 million deaths [6]. In many instances, COVID-19 can lead to pneumonia, often necessitating the hospitalization of those affected [7]. However, the two differ in several key aspects: pneumonia can be caused by various pathogens (bacteria, viruses, or fungi), while COVID-19 is specifically caused by the SARS-CoV-2 virus. Additionally, pneumonia is primarily treated based on its underlying cause (e.g., antibiotics for bacterial pneumonia), whereas COVID-19 treatments focus on antiviral therapies and supportive care. Moreover, vaccines exist for both, but they target different pathogens: pneumococcal vaccines for bacterial pneumonia and COVID-19 vaccines for SARS-CoV-2 [4,8].

The accurate diagnosis of both pneumonia and COVID-19 is crucial for effective treatment and patient outcomes. Early detection allows healthcare providers to determine the underlying cause, whether bacterial, viral, or fungal, and apply the appropriate treatment, such as antibiotics for bacterial pneumonia or antiviral care for COVID-19. Misdiagnosis or delayed diagnosis can lead to complications, prolonged illness, and increased mortality, particularly in vulnerable populations like children, the elderly, and those with weakened immune systems. Identifying the right disease ensures timely intervention and can significantly reduce the severity and spread of these infections [9,10].

In diagnosing both COVID-19 and pneumonia, several imaging tools are employed, each with distinct advantages and limitations. Chest X-rays (CXRs) are the most commonly used method due to their accessibility, affordability, and quick results, making them a valuable first-line diagnostic tool. However, they have lower sensitivity compared to computed tomography (CT) scans or magnetic resonance imaging (MRI). CT scans provide higher-resolution images, allowing for more detailed assessments of lung conditions but involve significantly higher radiation exposure and cost [5,11]. MRIs, while effective, are less frequently used for lung diseases due to longer scanning times and higher costs. CXRs, despite their limitations, remain crucial during COVID-19 surges as they enable rapid triaging alongside slower, gold-standard tests like reverse transcription-polymerase chain reaction (RT-PCR). The widespread use of CXRs also helps in resource-limited settings, although their lower resolution increases the risk of misinterpretation, particularly in areas lacking trained radiologists [5,11]. Computer-aided diagnosis (CAD) technologies can assist medical workers, including radiologists and physicians, in diagnosing pneumonia and COVID-19. Deep learning (DL) has been thoroughly explored as a CAD technique for diagnosing pneumonia [12-15] and COVID-19 [16-21]. For more detailed information, review studies (in 2024) on the use of deep learning methods in pneumonia diagnosis [22] and COVID-19 diagnosis [23] can be consulted.

According to data from Johns Hopkins University (latest update as of March 10, 2023), Turkey has recorded 17,042,722 COVID-19 cases and 101,492 deaths, indicating a significant mortality rate associated with this disease. We utilized chest X-ray (CXR) images from patients diagnosed with pneumonia, COVID-19, and healthy individuals to ensure automated diagnosis of these diseases through binary and multi-class classification using some deep learning architectures. Notably, our research distinguishes itself from previous works by not relying on custom models, ensuring a balanced dataset across the groups, and employing SqueezeNet for the first time in such comparisons. Additionally, we achieved a pioneering classification of pneumonia versus normal and COVID-19 versus pneumonia within this dataset,

underscoring the significance of our contributions to the field of medical imaging and disease diagnosis. Figure 1 illustrates the workflow of the study.

The original contributions of this study differ from existing approaches in the literature in several important ways. First, it addresses two specific binary classification scenarios not found in most similar studies: the distinction between COVID-19 and pneumonia, and the classification of normal and pneumonia. These additional classification tasks enable a more comprehensive evaluation of the differential diagnosis process, which is particularly critical from a clinical perspective. Second, the study used a larger and more balanced CXR dataset than many literature studies, thereby increasing the generalizability of the models. Third, the use of lightweight deep learning architectures such as AlexNet and SqueezeNet provides a significant advantage in terms of evaluating the applicability of these models in real-time and resource-limited clinical settings due to their low hardware requirements. Finally, model performance was reported as the mean ± standard deviation across multiple runs, rather than based on a single run, thus emphasizing model stability. In this respect, the study draws attention to consistency assessment, which is often overlooked in the literature.

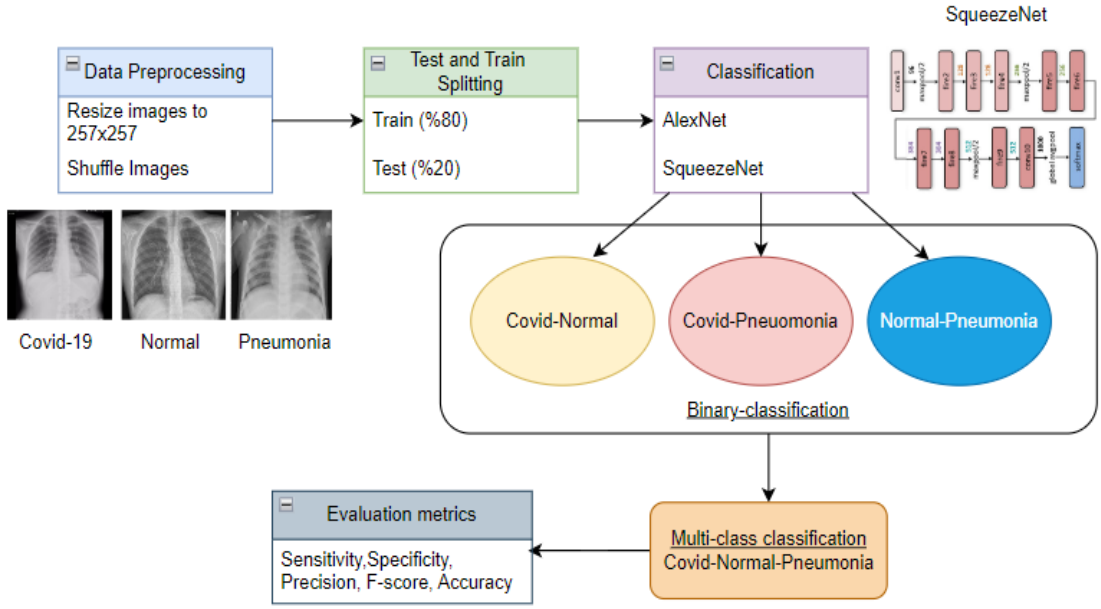

Figure 1. Flowchart of the study

2. MATERIAL AND METHOD

In this section, the dataset used, Convolutional Neural Network (CNN) architectures, and classification results were explained.

2.1. Data Description

The dataset consists of chest CXR images organized into three distinct categories: COVID-19, normal, and pneumonia. It includes a total of 1626 COVID-19 images, 1802 normal images, and 1800 pneumonia images. All images have been preprocessed and resized to 256x256 pixels in PNG format, ensuring uniformity for analysis [24]. This dataset, available as open access at "https://data.mendeley.com/datasets/dvntn9yhd2/1", serves as a valuable resource for researchers and the medical community, facilitating the development of deep learning models for the automatic detection and classification of COVID-19 and pneumonia from CXR images. Figure 2 depicts the distribution of images used in the multi-class and binary classification tasks. In the multi-class setting, the dataset is balanced across the three categories, with 31% COVID-19, 34% pneumonia, and 35% normal images. For the binary task (COVID-19 vs. normal), the distribution is also balanced, consisting of 47% COVID-19 and 53% normal CXR images. In the other binary task (pneumonia vs. normal), the dataset is perfectly balanced, with each class representing 50% of the images. This balanced distribution promotes accurate model training and reduces class bias during evaluation. Figure 3 depicts some images from the dataset.

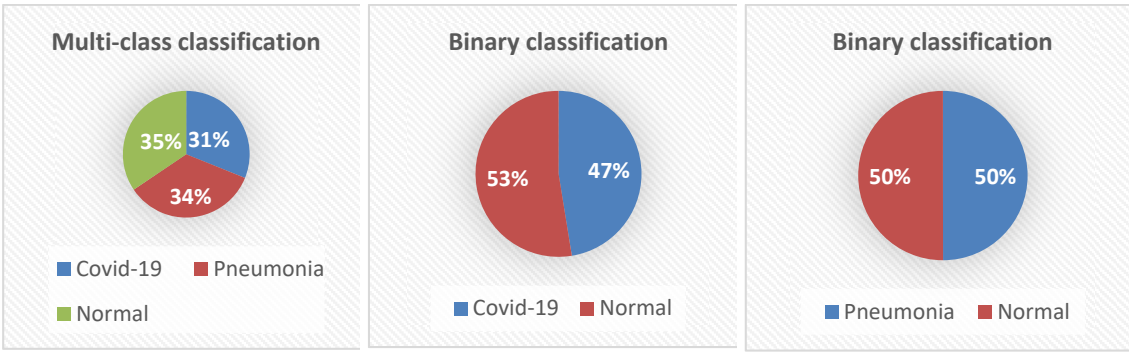

Figure 2. Visualization of data distribution for binary and multi-class tasks

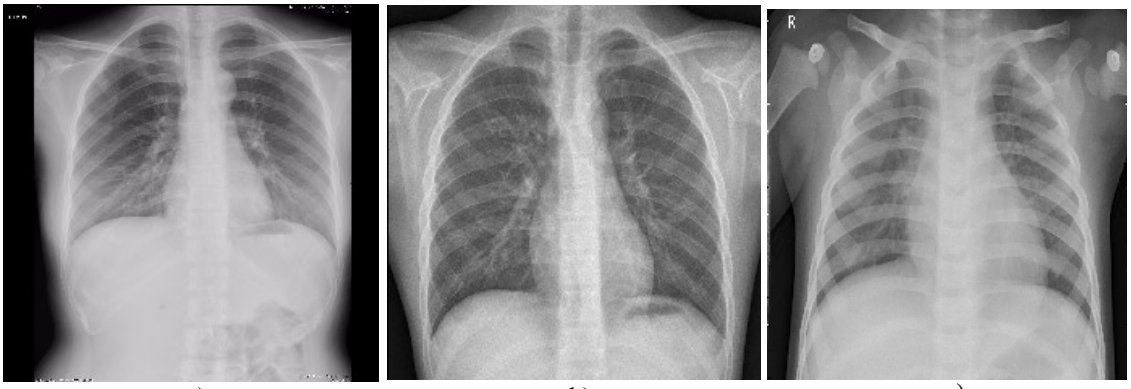

a) b) c)

Figure 3. Sample CXR images from the dataset a) for Covid-19 b) for Normal c) for Pneumonia

2.2. CNN Architectures

In this study, AlexNet and SqueezeNet deep learning architectures were used to classify images. AlexNet was introduced by Krizhevsky et al. [25] in the year 2012. Later on, it won the ImageNet Large Scale Visual Recognition Challenge (ILSVRC) of the same year. This architecture is mainly composed of several layers: five convolutional layers, three fully connected layers, five max-pooling layers, and a final SoftMax layer. It also incorporates ReLU activations and dropout mechanisms to make the model even stronger. This neural network requires input dimensions of 227×227×3. In convolutional layers, features from the input are extracted; a key feature of convolution is that filters (often referred to as kernels) are applied and moved over the input to produce feature maps. Furthermore, pooling layers serve to decrease both the dimensionality and the complication of data in order to enhance efficiency in computational terms through downsampling to retain only the most significant features. Pooling layers normally come after convolutional or fully connected layers. The fully connected layers flatten the 2D feature maps to a one-dimensional matrix-a pathway to data classification.

SqueezeNet is a small deep model trained to provide state-of-the-art performance with many fewer parameters than the larger models like AlexNet. Iandola and his team, in the year 2016, came up with SqueezeNet [26]. The main idea behind SqueezeNet was making it compact and efficient without affecting the accuracies, which really helps the systems with low computational resources. The core idea behind SqueezeNet involves something called the "fire module," a building block that greatly reduces network complexity. In its approach, it first uses a "squeeze" layer with 1x1 filters to reduce the amount of data in the flow, then an "expand" layer which combines both 1x1 and 3x3 filters in order to recover the information at a more detailed level. This method greatly reduces the number of parameters while still being able to find important features within images. The model also replaces the fully connected layers with global average pooling, which again increases its space efficiency. Despite its very compact design, the SqueezeNet demonstrates remarkable performance in image classification tasks and hence should be among the top candidates for resource-constrained platforms such as mobile devices and embedded systems.

AlexNet and SqueezeNet have huge differences in regard to size and efficiency of operation. While AlexNet has around 60 million parameters and requires about 240 MB of memory, SqueezeNet presents a much smaller framework with only 1.2 million parameters and 5 MB for the model size [27]. Such high reduction is possible by using 1x1 convolutions and introducing the "fire module," which includes 1x1 and 3x3 convolutions to keep the effectiveness of feature extraction high. Besides that, Sreplaces fully connected layers with global average pooling, reduces over-fitting, and further reduces the size of the model. While AlexNet is optimized for high accuracy on larger datasets, SqueezeNet is optimized for memory-constrained environments and therefore is very well-suited for mobile and embedded devices [27].

To train the model, we employ deep learning methods with a batch size of 16 using categorical cross-entropy as the loss function. A validation set is used during training to improve accuracy by fine-tuning model parameters. The dataset was trained for 12 epochs, as preliminary experiments showed that accuracy improved and both training and validation losses reached a saturation point within this range, enabling efficient training and high predictive performance without overfitting.

Table 1. The fundamental parameters of AlexNet and SqueezeNet

Parameter	AlexNet	SqueezeNet
Number of layers	8	18
Connected layers	3 fully connected layers	1 global average pooling layer
Activation function	ReLU	ReLU
Optimizer	Adam	Adam
Learning rate	0.0001	0.0001
Dropout	0.5	0.5
Batch size	128	128
Loss function	Cross-entropy	Cross-entropy

2.3. Model Comparison Metrics

5-fold cross-validation was used for training and testing the data. The evaluation of network performance was carried out using several key metrics: accuracy, sensitivity, specificity, precision, and F-score. These metrics were derived from the confusion matrix, illustrated in Table 2. TP designates images correctly classified as COVID-19, FP shows the number of images incorrectly categorized as COVID-19, TN includes images correctly classified as healthy and pneumonia, and FN gives the number of images that were incorrectly categorized as COVID-19 but were, in fact, healthy and pneumonia. All metric calculations were given in Equations (1)-(5). The experiments were performed on a laptop equipped with an Intel Core i5-9300H 8-core CPU running at 2.4 GHz, 16 GB of RAM, and a 4 GB Nvidia GeForce GTX 1650 graphics card.

Table 2. Confusion matrix for COVID-19 class (multi-class classification)

		Predicted class		
		Normal	COVID-19	Pneumonia
Actual class	Normal	TN	FP	TN
	COVID-19	FN	TP	FN
	Pneumonia	TN	FP	TN

$$\text{Sensitivity} = \frac{\text{TP}}{\text{TP+FN}} \quad (1)$$

$$\text{Specificity} = \frac{\text{TN}}{(\text{TN+FP})} \quad (2)$$

$$\text{Precision} = \frac{TP}{TP+FP} \quad (3)$$

$$\text{F} - \text{Score} = \frac{2\text{TP}}{2\text{TP+FP+FN}} \quad (4)$$

$$\text{Accuracy} = \frac{(\text{TP+TN})}{(all\ predictions)} \quad (5)$$

3. RESULTS

In this section, binary classification and multi-class classification results performed with AlexNet and SqueezeNet were given. Table 3 presents the performance metrics for three different binary classifications: Covid-Normal, Covid-Pneumonia, and Normal-Pneumonia, using AlexNet and SqueezeNet. The performance metrics include sensitivity, specificity, precision, F-score, and accuracy. For the Covid-Normal classification, AlexNet achieved an accuracy of 99.42%, while SqueezeNet outperformed it with an accuracy of 99.85%. In the Covid-Pneumonia classification, AlexNet produced an accuracy of 98.51%, whereas SqueezeNet again demonstrated superior performance with 99.85% accuracy. Finally, for the Normal-Pneumonia classification, AlexNet reached an accuracy of 96.25%, while SqueezeNet outperformed it with 98.08%.

Table 3. Binary classification results (%)

binary classification	Method	sensitivity	specificity	precision	F-score	accuracy
Covid-normal	AlexNet	99.69	99.18	99.08	99.38	99.42
	SqueezeNet	99.82	99.89	99.88	99.85	99.85
Covid-pneumonia	AlexNet	98.53	98.58	98.40	98.44	98.51
	SqueezeNet	99.88	99.83	99.82	99.85	99.85
Normal-pneumonia	AlexNet	96.18	96.55	96.45	96.26	96.25
	SqueezeNet	97.82	98.40	98.39	98.09	98.08

SqueezeNet consistently achieved higher results across all classification tasks compared to AlexNet, particularly in the Covid-Normal and Covid-Pneumonia categories, where it excelled with accuracy levels of 99.85% in both cases. The difference is most notable in the Normal-Pneumonia classification, where SqueezeNet achieved 98.08% accuracy, outperforming AlexNet's 96.25%. These results indicate that SqueezeNet is more efficient for binary classification in this context, with a smaller network that offers faster computations without compromising on classification performance. In Figures 4 and 5, confusion matrices for each fold of the Covid-Normal binary classification were given.

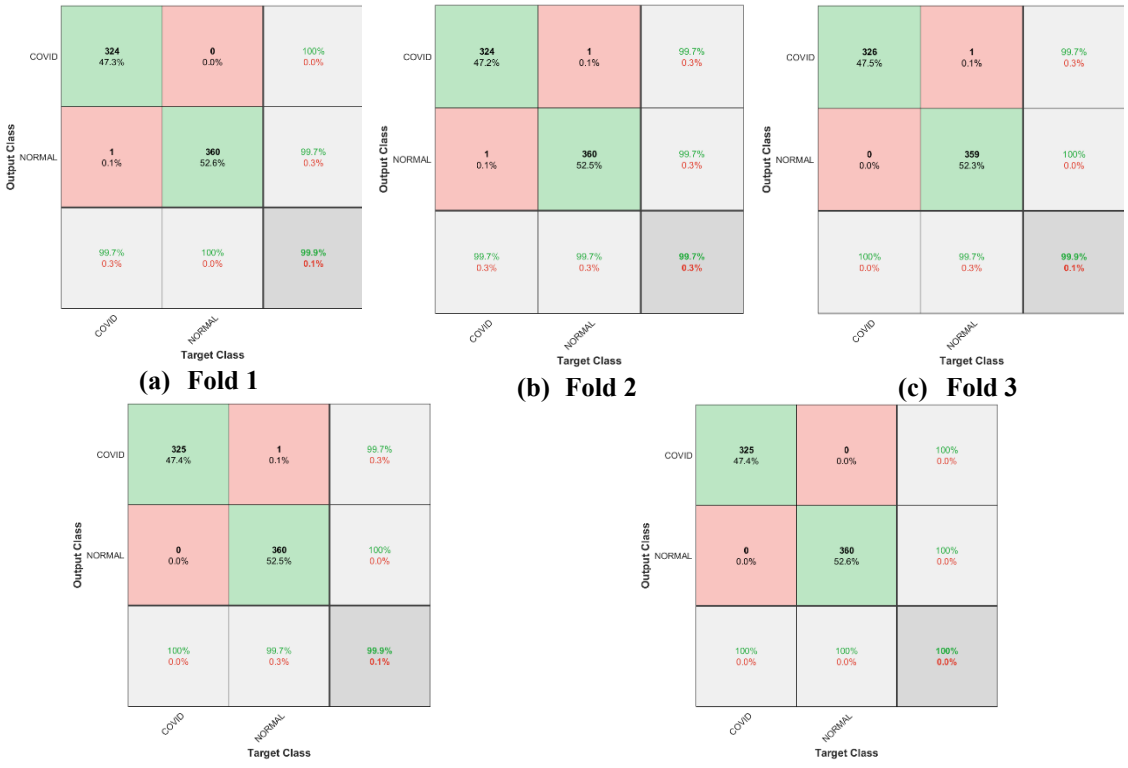

(a) Fold 1 **(b) Fold 2** **(c) Fold 3**

(d) Fold 4 **(e) Fold 5**

Figure 4. Confusion matrices for each fold (a–e) of the 5-fold cross-validation in COVID-Normal classification using SqueezeNet

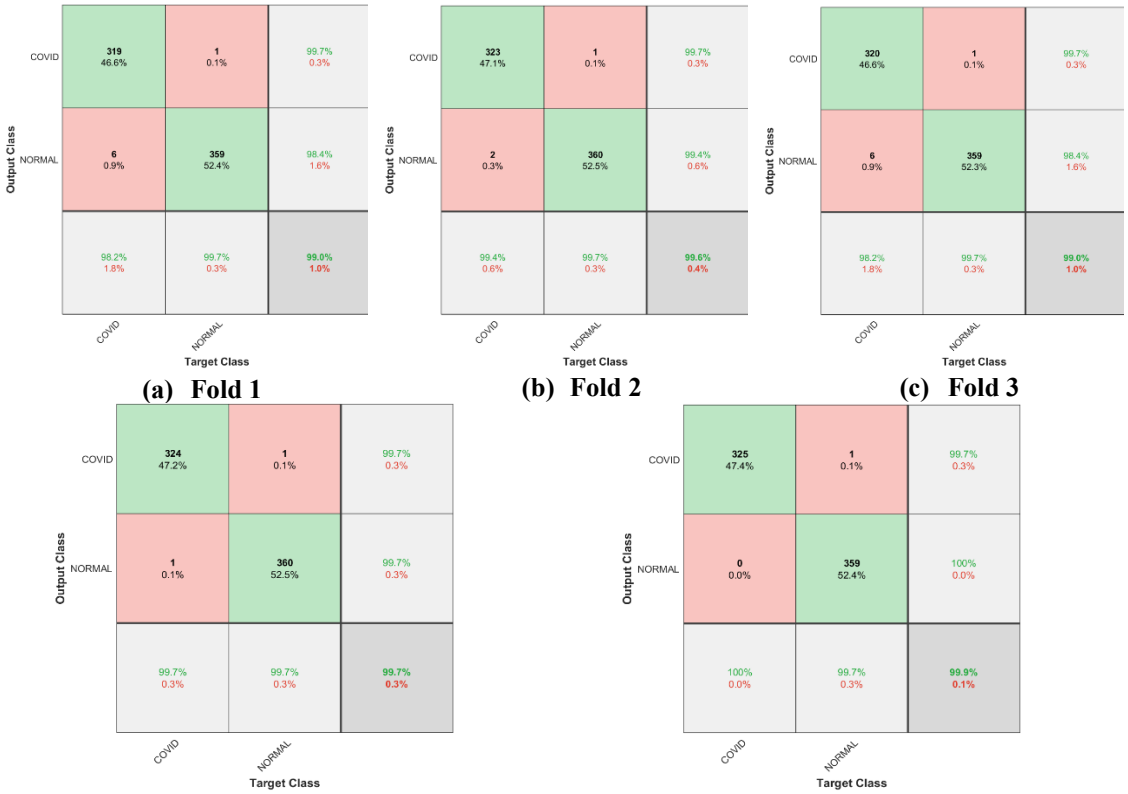

Figure 5. Confusion matrices for each fold (a–e) of the 5-fold cross-validation in COVID-Normal classification using AlexNet

Figure 6 shows the visualization of the standard deviation of the results obtained 5-fold in binary classification. The standard deviation values for each metric (sensitivity, specificity, precision, F-score, and accuracy) show considerable variation across the models and tasks. Higher standard deviation values suggest more variation in model performance over folds. For example, AlexNet's sensitivity for the COVID-Pneumonia and Normal-Pneumonia tasks varies significantly, implying that its predictions for these classes may be unstable. In contrast, SqueezeNet performs better consistently, particularly for COVID-Normal classification.

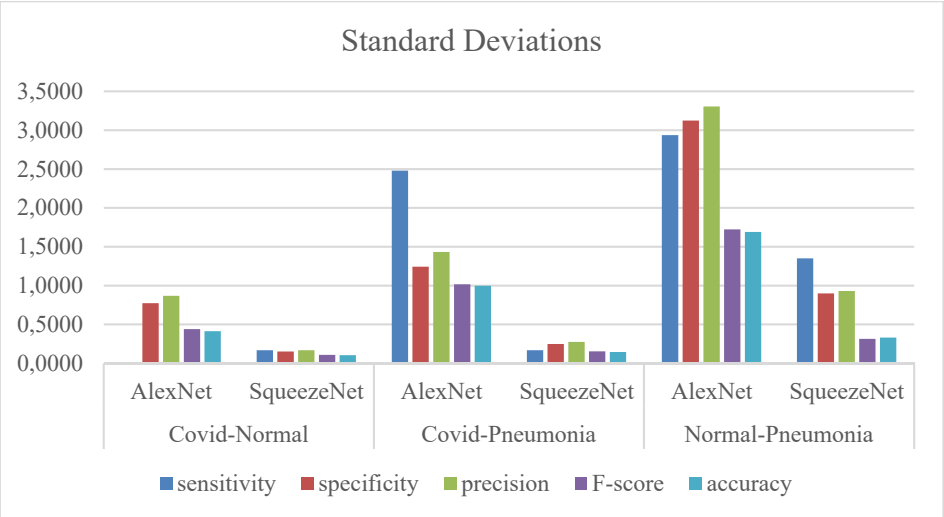

Figure 6. Standard deviations of classification performance metrics across each fold for each binary classification task (COVID-Normal, COVID-Pneumonia, and Normal-Pneumonia) using AlexNet and SqueezeNet models

To explain in more detail, for Covid-Normal classification, AlexNet demonstrated a sensitivity standard deviation of 0.0025, indicating stable sensitivity, but had a higher standard deviation for specificity (0.7740), precision (0.8688), F-score (0.4387), and accuracy (0.4126), suggesting more fluctuations in these areas. SqueezeNet, on the other hand, showed much larger variability, especially in sensitivity (0.1680) and specificity (0.1517), indicating a less stable performance. In the Covid-Pneumonia classification, AlexNet showed relatively higher standard deviations across all metrics, with sensitivity at 2.4800 and specificity at 1.2440, indicating significant fluctuations. SqueezeNet also exhibited lower stability, with sensitivity at 0.1683 and specificity at 0.2473.

Finally, for Normal-Pneumonia classification, AlexNet again showed large standard deviations, with sensitivity at 2.9364 and specificity at 3.1238, reflecting substantial variance in model performance. SqueezeNet showed slightly less variability but still had high standard deviations for metrics like sensitivity (1.3493) and specificity (0.8998). The results indicate that AlexNet generally exhibits more variance in performance, particularly in sensitivity and specificity across all binary classification tasks. SqueezeNet shows slightly better stability in comparison, but still has relatively high standard deviations, especially for precision and F-scores. These findings suggest that while both models can achieve high accuracy, their performance may vary significantly, especially under different test conditions, making it crucial to interpret results with consideration of these variations. Figure 7 shows the confusion matrices for each fold of SqueezeNet, whose average accuracy for multiple classification is 97.72%.

Table 4. Multi-class classification results (%)

Multi-class classification	**Method**	**sensitivity**	**specificity**	**precision**	**F-score**	**accuracy**
Covid-normal-pneumonia	AlexNet	97.44	98.68	97.37	97.39	97.36
	SqueezeNet	97.88	98.88	97.78	97.78	97.72

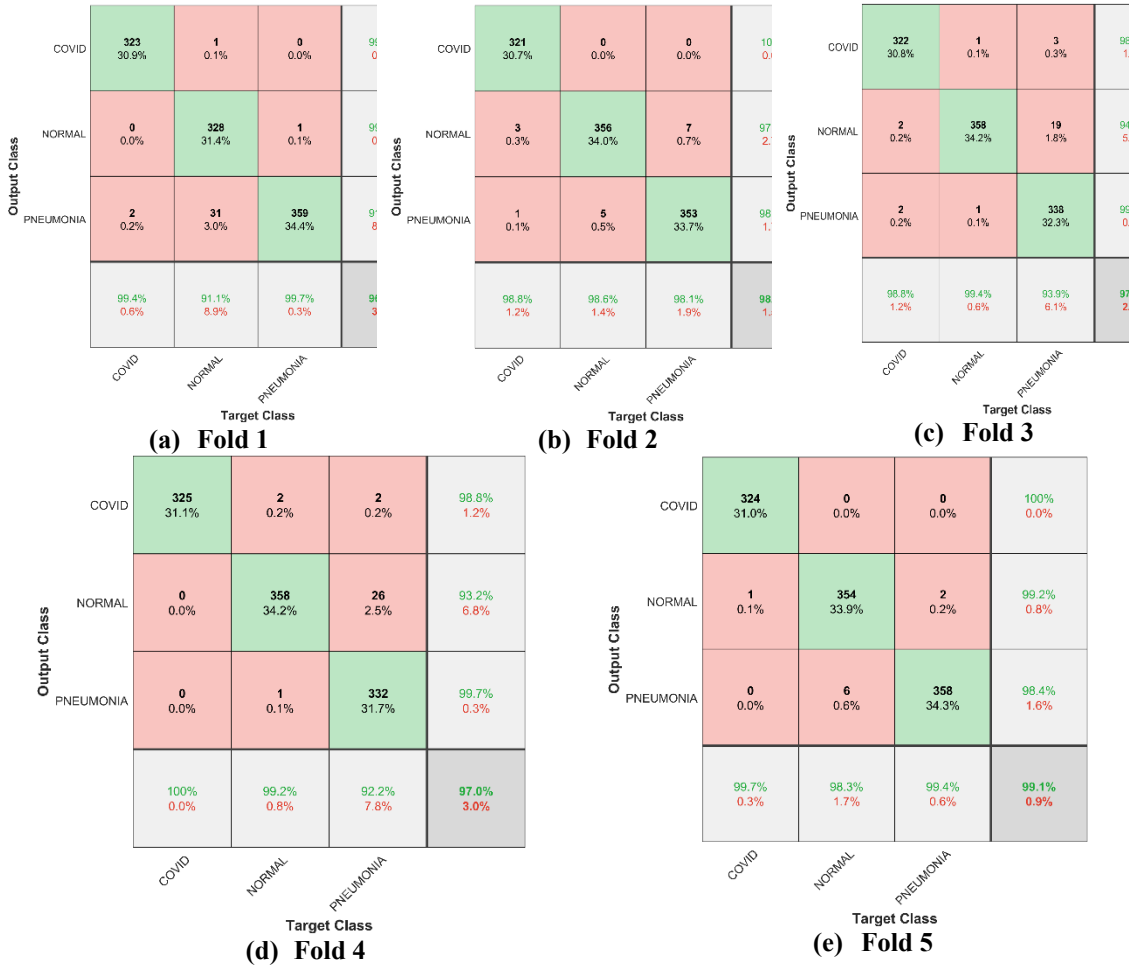

Figure 7. Confusion matrices for each fold (a–e) of the 5-fold cross-validation in COVID-Normal-Pneumonia (multi-class) classification using SqueezeNet

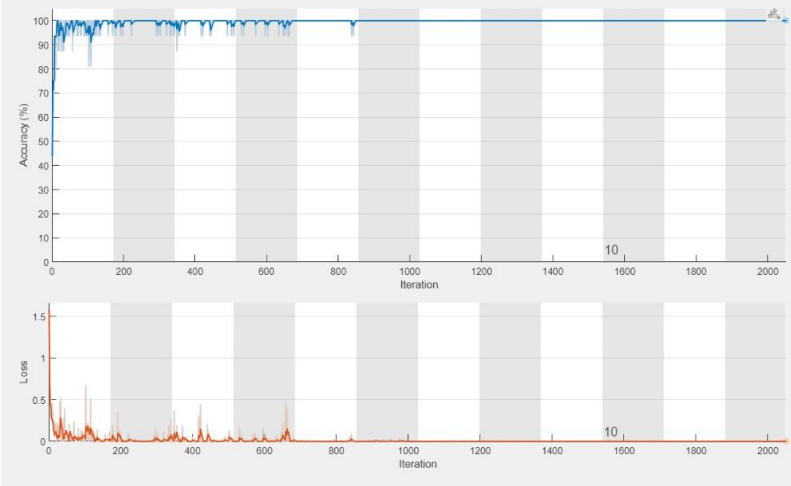

Figure 8. SqueezeNet training process in Covid-Normal classification

Table 4 presents the performance of AlexNet and SqueezeNet in a multi-class classification task involving Covid-Normal-Pneumonia. AlexNet achieved an accuracy of 97.36%, with a sensitivity of 97.44%, specificity of 98.68%, precision of 97.37%, and an F-score of 97.39%. On the other hand, SqueezeNet slightly outperformed AlexNet, achieving an accuracy of 97.72%, with a sensitivity of 97.88%, specificity of 98.88%, precision of 97.78%, and an F-score of 97.78%.

In summary, while both models performed exceptionally well, SqueezeNet showed marginally better results in all evaluation metrics. This demonstrates that SqueezeNet not only maintains high levels of accuracy in multi-class classification but also offers slightly improved sensitivity and specificity compared to AlexNet. These results highlight the potential of SqueezeNet for more accurate classification in complex tasks such as detecting COVID-19, normal, and pneumonia cases simultaneously.

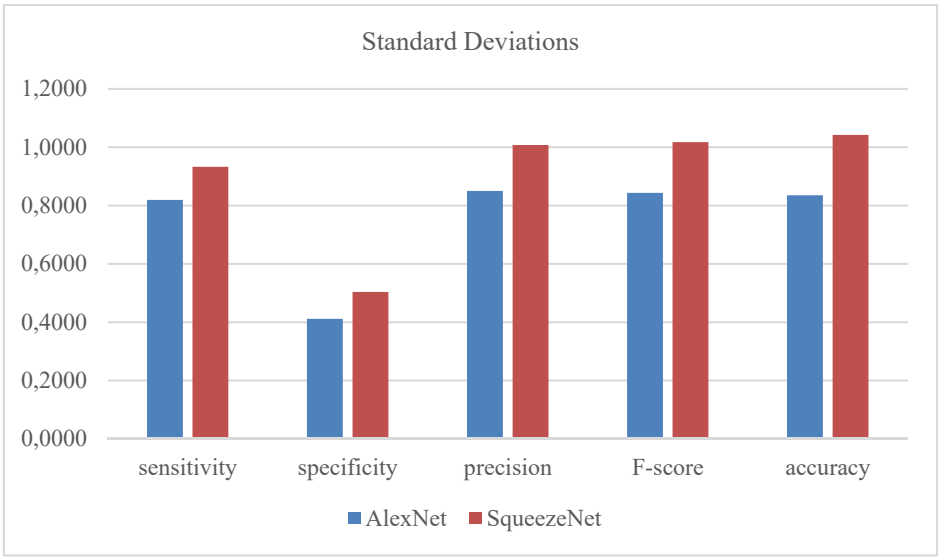

Figure 9. Standard deviations of performance metrics across each fold in the multi-class classification task

Figure 8 depicts how SqueezeNet quickly achieves excellent accuracy at low epoch values. Figure 9 displays the standard deviations of five key performance metrics—sensitivity, specificity, precision, F-score, and accuracy—obtained from 5-fold cross-validation for the multi-class classification task using AlexNet and SqueezeNet models. Each bar in the graph reflects the degree of variability in a particular metric between folds. The standard deviation values reflect the consistency of each model's performance during cross-validation. Lower standard deviations indicate more stable and reliable classification results, while higher values suggest greater fluctuation in the model's predictions. AlexNet has significant

variability across measurements, with the maximum standard deviation in precision and accuracy being about 0.8-0.85. However, SqueezeNet exhibits slightly higher variability, particularly in precision and F-score, with deviations greater than 1.0, indicating more irregularity in its predictions and overall performance. Both models exhibit performance swings, with SqueezeNet having a somewhat larger variance across most metrics than AlexNet. SqueezeNet's greater standard deviations in precision, F-score, and accuracy suggest that its multi-class classification performance is less stable. In contrast, AlexNet is slightly more stable, but still has substantial variability. These variances show the significance of take standard deviation into account when evaluating model performance, as high accuracy alone may not produce consistent results across different data subsets.

The standard deviation analysis reveals that while both models can effectively classify chest X-ray images, AlexNet offers more reliable performance with less fluctuation across validation folds. In contrast, SqueezeNet's higher variation suggests it may be more sensitive to changes in the dataset, which could affect its generalization capabilities in real-world applications.

4. DISCUSSION

CT scans and CXR images are appropriate for identifying lung problems in many countries because patients may receive them promptly and at a low cost. Many studies have employed chest radiographs to detect COVID-19 or pneumonia. Tuncer et al. [28] proposed an intelligent computer vision method for automatic COVID-19 detection from X-ray images, using a novel Residual Exemplar Local Binary Pattern (ResExLBP) for feature extraction and iterative ReliefF for feature selection. The method achieved 100% accuracy with the SVM classifier using 10-fold cross-validation, demonstrating its high effectiveness in Covid-19 diagnosis. However, since 87 Covid-19 CXR images and 234 healthy CXR images were used in this study, there is data imbalance and image scarcity. Khalifa et al. [29] proposed a pneumonia detection method from CXR using generative adversarial networks (GAN) combined with fine-tuned deep transfer learning models. By using GAN to augment the dataset, the model avoided overfitting and generated additional training images, allowing the use of only 10% of the original dataset. ResNet18, AlexNet, GoogLeNet, and SqueezeNet were selected for their lower complexity, with ResNet18 achieving the best performance, including 99% accuracy, precision, recall, and F1 score. The study outperformed related work despite using a smaller portion of the dataset for training. Alshmrani et al. [30] proposed a deep learning architecture for multi-class classification of lung diseases, including COVID-19, pneumonia, lung cancer, tuberculosis (TB), and lung opacity, using CXR images. The model utilized a pre-trained VGG19 combined with three blocks of CNN for feature extraction and classification. The model achieved remarkable performance with 96.48% accuracy, 93.75% recall, 97.56% precision, 95.62% F1 score, and 99.82% AUC. Li et al. [31] proposed a hybrid deep neural network, COVID19-ResCapsNet, for the detection of COVID-19 from chest X-ray images. The model combines an improved Residual feature extraction network and Capsule Networks to classify COVID-19 and non-COVID-19 cases. Evaluated on two datasets (4236 and 2250 images), COVID19-ResCapsNet achieved impressive classification accuracies of 99.88% and 99.33%, respectively. The study also explored the impact of different optimizers and batch sizes, demonstrating the model's effectiveness as a supplementary diagnostic tool in clinical settings. Additionally, in the second dataset containing 750 pneumonia, 750 non-COVID and 750 COVID-19 CXR images, 99.11% accuracy was achieved with COVID19-ResCapsNet and 98.19% accuracy was achieved with ResNet-101 in multi-class classification.

Ali et al. [32] explored the application of deep learning algorithms in medical imaging, particularly using X-rays for diagnosing conditions like lung cancer, bone fractures, COVID-19, and pneumonia. Their custom deep learning model achieved 97.96% accuracy in classifying the dataset equally among healthy, COVID, and pneumonia patients. Also, they conducted experiments using pre-trained DenseNet201, XceptionNet, and MobileNet models for classifying medical conditions from CXR images. The XceptionNet model showed a validation accuracy of 95.53% and a test accuracy of 92.90%. The classification results were reported across training, testing, and validation phases, demonstrating the robustness of the model for medical image analysis. Kumar et al. [33] propose a deep neural network-based model called "LiteCovidNet" for detecting COVID-19 and pneumonia cases using CXR images. The model performs both binary classification (COVID-19 vs. Normal) and multi-class classification (COVID-19, Normal, Pneumonia). It achieves an impressive accuracy of 100% for binary classification and 98.82% for multi-class classification, demonstrating competitive performance compared to other recent studies. Shastri et al. [34] introduced the CheXImageNet model for detecting COVID-19 from digital chest X-ray images

using an open-access dataset. The study achieved a remarkable 100% accuracy for both binary classification (COVID-19 vs. normal X-ray) and multi-class classification (COVID-19, normal X-ray, and pneumonia). While these results are promising, the authors acknowledge that further work is required to enhance the model's robustness. They aim to expand the dataset with more COVID-19 cases and extend their method to digital CT images. Additionally, future work will focus on developing automated tools or software using multi-modality deep learning models, including CT scans and X-rays, for more accurate detection in noisier environments. The authors also plan to explore deeper neural networks to handle larger datasets and improve classification performance. While the study reports 100% accuracy in both binary and multi-class classification, there are some aspects that warrant further discussion. The custom model's validity, when compared to well-established architectures like AlexNet, may be questioned due to the lack of extensive testing on larger datasets. Additionally, the study does not provide details about the training time or computational cost of the algorithm, which are crucial factors in assessing its practical applicability. Therefore, while the results are promising, the generalizability and efficiency of the model need to be further evaluated. Also, The CheXImageNet architecture, with its 27 layers, may introduce a computational load, particularly depending on the available hardware resources like the GPU or CPU. Layers such as convolutional layers with larger filters (32, 64, 256 filters) and activation functions like LeakyReLU can increase the number of trainable parameters, thus adding to the complexity. The input image size also plays a role in determining the overall load. While 27 layers are moderate in size for deep learning models, modern hardware and optimized implementations can manage this efficiently, though it may still impact performance on less powerful systems. Marques et al. [35] proposed an automated diagnosis system for COVID-19 using the EfficientNet model on CXR images. The study employed a 10-fold cross-validation approach and conducted both binary and multi-class classification. In the multi-class task (COVID-19, Pneumonia, Normal), the model achieved an accuracy of 96.70%, while in binary classification (COVID-19 vs. Normal), it achieved 99.62% accuracy. However, the dataset used in this study was relatively small, which may limit the generalizability and robustness of the results. The model showed reasonable performance, but the work did not evaluate other diagnostic challenges, such as distinguishing COVID-19 from pneumonia. Ebenezer et al. [36] investigated the effect of image transformation techniques on EfficientNet performance for classifying COVID-19 from CT scan images. The study achieved an accuracy of 94.56% for binary classification. Although it demonstrated that pre-processing improves performance, it focused solely on CT data and did not evaluate chest X-rays or explore the classification between pneumonia and other conditions. Sharma and Sharma [37] presented a binary classification method for identifying COVID-19 from CT scan images using the EfficientNet model. The study reported a training accuracy of 99.54% and a test accuracy of 98.24%, indicating strong performance in distinguishing COVID-19 from non-COVID cases. However, the study did not include multi-class classification and focused exclusively on CT images without evaluating performance on CXR images or considering lightweight architectures. In comparison, our study used a larger and balanced dataset, achieving 99.85% accuracy in binary classification (COVID-19 vs. Normal) and 97.72% accuracy in multi-class classification using the lightweight SqueezeNet model.

According to binary classification, SqueezeNet consistently delivered higher results in all categories compared to AlexNet. It achieved notably better sensitivity, specificity, and accuracy, especially in the Covid-Normal and Covid-Pneumonia classifications. SqueezeNet's performance highlights its efficiency in binary classification tasks, with a smaller model architecture that offers computational advantages without sacrificing accuracy. This makes it a more suitable option for rapid and accurate diagnostic applications. SqueezeNet is suitable for portable X-ray and low-end environments, enabling fast inference on mobile and embedded clinical devices thanks to its low number of parameters (~1.2M) and small model size (~5MB). AlexNet, on the other hand, is preferred as a reference model in clinical research requiring high accuracy due to its larger capacity and powerful transfer learning capability [26].

In our study, instead of using a custom model, AlexNet and SqueezeNet were employed, achieving an accuracy of 99.85% for binary classification (Covid-Normal, Covid-Pneumonia) using SqueezeNet and an accuracy of 97.72% for multi-class classification using SqueezeNet. This result demonstrates the effectiveness of these well-established deep learning architectures in the detection of COVID-19, offering a competitive performance compared to other models such as "LiteCovidNet" and similar studies that report 100% accuracy. However, a key distinction in our research lies in the unique binary classifications performed: pneumonia vs. COVID-19 and pneumonia vs. healthy. These additional classification tasks, not present in many other studies, further showcase the versatility and robustness of the proposed approach in distinguishing between complex conditions, potentially enhancing diagnostic precision for healthcare

professionals. Table 5 presents representative deep learning–based studies that report binary and multi-class classification results for COVID-19 and pneumonia using CXR datasets of comparable scale, highlighting studies that are widely referenced in the literature. In the study conducted by Ucar [38] and Chowdhury [39], AlexNet was not implemented; instead, data augmentation was employed to increase the image count and achieve class balance. Although Karakanis's study [40] attained high accuracy in multi-class classification, its dataset was balanced but relatively small. Our study, on the other hand, benefits from a larger and balanced dataset, enhancing the robustness of the findings. Furthermore, a unique contribution of this work is the inclusion of specific binary classification tasks (COVID-19 vs. pneumonia and normal vs. pneumonia), which, combined with multi-class classification, yielded high accuracy. These distinctions underscore the efficacy and comprehensive nature of our approach compared to existing studies. Our findings were also compared with the recent study by Singh et al. [41], which used the same dataset. Unlike their Deep CP-CXR model, which is computationally heavier and limited to a single binary task (COVID-19 vs. pneumonia), our approach employs lightweight architectures, performs multiple binary and multi-class classifications, and reports results with stability analysis. These aspects make our method more efficient, broader in scope, and more suitable for real-time clinical applications.

Table 5. Comparison with other studies

Author	Data	Method	Binary classification results	Multi-class classification results
Kumar et al. [33]	1475 normal, 1480 pneumonia and 1281 COVID-19 CXR images	Custom CNN model named LiteCovidNet	(COVID-19 and normal) 100% accuracy	98.82% accuracy
Shastri et al. [34]	358 normal, 340 pneumonia and 347 COVID-19 CXR images	Custom CNN model named CheXImageNet	(COVID-19 and normal) 100% accuracy	100% accuracy
Ucar et al. [38]	1583 normal, 4290 pneumonia and 76 COVID-19 CXR images	Bayes-SqueezeNet	NA	98.3% accuracy
Chowdhury et al. [39]	1579 normal, 1485 pneumonia and 423 COVID-19 CXR images	DenseNet201 and SqueezeNet	(COVID-19 and normal) 99.70% weighted accuracy using DenseNet201 and %99.40 weighted accuracy using SqueezeNet	97.94% weighted accuracy using DenseNet201 and 95.10% weighted accuracy using SqueezeNet
Karakanis and Leontidis [40]	275 normal, 275 pneumonia and 275 COVID-19 CXR images	Custom CNN model	(COVID-19 and normal) 98.7% accuracy	98.3% accuracy
Apostolopoulos and Mpesiana [42]	504 normal, 714 pneumonia and 224 COVID-19 CXR images	MobileNetv2	(COVID-19 and normal) 96.78% accuracy	94.72% accuracy
Aljuaid et al. [43]	2313 CXR images for each class (COVID-19, normal and pneumonia)	Several CNN models	NA	97% accuracy using VGG-19
Singh et al. [41]	1802 normal, 1800 pneumonia, and 1626 COVID-19 CXR images	Deep CP-CXR, Custom CNN model	100% accuracy (COVID-19 and normal)	98.57% accuracy
Randieri et al. [44]	5017 CXR images for each class (COVID-19, normal and pneumonia)	Custom CNN model	NA	97.48% accuracy
Proposed study	1802 normal, 1800 pneumonia, and 1626 COVID-19 CXR images	AlexNet SqueezeNet	COVID-19 and normal 99.85% accuracy, COVID-19 and pneumonia 99.85% accuracy, Normal and pneumonia 98.08% accuracy using SqueezeNet	97.72% accuracy using SqueezeNet

5. CONCLUSIONS

This work highlights the effectiveness of AlexNet and SqueezeNet in automatically classifying chest X-ray images into COVID-19, pneumonia, and healthy categories, achieving a maximum binary classification accuracy of 99.85%. While AlexNet provided consistent performance across all metrics, SqueezeNet, though accurate on average, displayed greater variation in precision and F-score. The study employed a rigorous 5-fold cross-validation framework for the three-class problem, including per-fold confusion matrices and stability analyses, ensuring a thorough assessment of model reliability. These results demonstrate the practical potential of automated diagnostic tools, especially in settings with limited clinical resources. Although the dataset was balanced across groups and larger than those in many previous studies, it was obtained from a single source, which may limit generalizability. Future studies will focus on applying these models to heterogeneous datasets, including CT images, to further evaluate generalizability and enhance diagnostic support for respiratory conditions.

6. DATA AVAILABILITY

The X-Ray images used in this study are openly available at Mendeley data repository [https://data.mendeley.com/datasets/dvntn9yhd2/1]

7. REFERENCES

1. Schwarz, M.I. & King, T.E. (2003). *Interstitial lung disease*. PMPH-USA, 5th Edition, 1151.
2. Abut, S. (2024). AI-based model design for prediction of COPD grade from chest X-ray images: a model proposal (COPD-GradeNet). *Çukurova Üniversitesi Mühendislik Fakültesi Dergisi*, *39*(2), 325-338.
3. Huang, C., Wang, Y., Li, X., Ren, L., Zhao, J., Hu, Y., Zhang, L., Fan, G., Xu, J., Gu, X., Cheng, Z., Yu, T., Xia, J., Wei, Y., Wu, W., Xie, X., Yin, W., Li, H., Liu, M., Xiao, Y., Gao, H., Guo, L., Xie, J., Wang, G., Jiang, R., Gao, Z., Jin, Q., Wang, J. & Cao, B. (2020). Clinical features of patients infected with 2019 novel coronavirus in Wuhan, China. *The lancet, 395*(10223), 497-506.
4. World Health Organization (WHO), (2024). *Pneumonia in children.* (https://www.who.int/), Access date: October 2024.
5. Siddiqi, R. & Javaid, S. (2024). Deep learning for pneumonia detection in chest x-ray images: A comprehensive survey. *Journal of Imaging, 10*(8), 176.
6. Johns Hopkins University & Medicine, Johns Hopkins Coronavirus Resource Center. (https://coronavirus.jhu.edu/), Access date: October 2024.
7. Ieracitano, C., Mammone, N., Versaci, M., Varone, G., Ali, A., Armentano, A., Calabrese, G., Ferrarelli, A., Turano, L., Tebala, C., Hussain, Z., Sheikh, Z., Sheikh, A., Sceni, G., Hussain, A. & Morabito, F. (2022). A fuzzy-enhanced deep learning approach for early detection of Covid-19 pneumonia from portable chest X-ray images. *Neurocomputing, 481*, 202-215.
8. Centers for Disease Control and Prevention (CDC) (2024). *COVID-19: Clinical care.* (https://archive.cdc.gov/), Access date: October 2024.
9. Anderson, R. & Feldman, C. (2023). The global burden of community-acquired pneumonia in adults, encompassing invasive pneumococcal disease and the prevalence of its associated cardiovascular events, with a focus on pneumolysin and macrolide antibiotics in pathogenesis and therapy. *International Journal of Molecular Sciences, 24*(13), 11038.
10. Kim, P.S., Read, S.W. & Fauci, A.S. (2020). Therapy for early COVID-19: a critical need. *Jama, 324*(21), 2149-2150.
11. Rana, S., Hosen, M.J., Tonni, T.J., Rony, M.A.H., Fatema, K., Hasan, M., Rahman, M., Khan, R., Jan, T. & Whaiduzzaman, M. (2024). DeepChestGNN: A comprehensive framework for enhanced lung disease identification through advanced graphical deep features. *Sensors, 24*(9), 2830.
12. Kundu, R., Das, R., Geem, Z.W., Han, G.-T. & Sarkar, R. (2021). Pneumonia detection in chest X-ray images using an ensemble of deep learning models. *PloS one, 16*(9), e0256630.
13. Rajaraman, S., Guo, P., Xue, Z. & Antani, S.K. (2022). A deep modality-specific ensemble for improving pneumonia detection in chest x-rays. *Diagnostics, 12*(6), 1442.
14. Ibrahim, A.U., Ozsoz, M., Serte, S., Al-Turjman, F. & Yakoi, P.S. (2024). Pneumonia classification using deep learning from chest X-ray images during COVID-19. *Cognitive Computation, 16*(4), 1589-1601.

15. Jaiswal, A.K., Tiwari, P., Kumar, S., Gupta, D., Khanna, A. & Rodrigues, J.J.P.C. (2019). Identifying pneumonia in chest X-rays: A deep learning approach. *Measurement, 145*, 511-518.
16. Wang, L., Lin, Z.Q. & Wong, A. (2020). Covid-net: A tailored deep convolutional neural network design for detection of covid-19 cases from chest x-ray images. *Scientific Reports, 10*(1), 19549.
17. Mousavi, Z., Shahini, N., Sheykhivand, S., Mojtahedi, S. & Arshadi, A. (2022). COVID-19 detection using chest X-ray images based on a developed deep neural network. *SLAS Technology, 27*(1), 63-75.
18. Hussain, E., Hasan, M., Rahman, M.A., Lee, I., Tamanna, T. & Parvez, M.Z. (2021). CoroDet: A deep learning based classification for COVID-19 detection using chest X-ray images. *Chaos, Solitons & Fractals, 142*, 110495.
19. Ismael, A.M. & Şengür, A. (2021). Deep learning approaches for COVID-19 detection based on chest X-ray images. *Expert Systems with Applications, 164*, 114054.
20. Oğuz, Ç. & Yağanoğlu, M. (2022). Detection of COVID-19 using deep learning techniques and classification methods. *Information Processing & Management, 59*(5), 103025.
21. Kılıç, Ş. (2025). A novel multi-head attention framework for COVID-19 detection: Hybrid integration of MobileNet and VGG19 with enhanced feature learning. *Çukurova Üniversitesi Mühendislik Fakültesi Dergisi, 40*(3), 655-670.
22. Sharma, S. & Guleria, K. (2024). A systematic literature review on deep learning approaches for pneumonia detection using chest X-ray images. *Multimedia Tools and Applications, 83*(8), 24101-24151.
23. Shoeibi, A., Khodatars, M., Jafari, M., Ghassemi, N., Sadeghi, D., Moridian, P., Khadem, A., Alizadehsani, R., Hussain, S., Zare, A., Alizadeh Sani, Z., Khozeimeh, F., Nahavandi, S., Acharya, U. & Gorriz, J. (2024). Automated detection and forecasting of covid-19 using deep learning techniques: A review. *Neurocomputing*, 127317.
24. Kumar, S. (2022). *Covid19-pneumonia-normal chest X-ray images.* Mendeley Data, 1. (https://doi.org/10.17632/dvntn9yhd2.1), Access date: October 2024.
25. Krizhevsky, A., Sutskever, I. & Hinton, G.E. (2012). Imagenet classification with deep convolutional neural networks. *Advances in Neural Information Processing Systems*, 25.
26. Iandola, F.N., Han, S., Moskewicz, M.W., Ashraf, K., Dally, W.J. & Keutzer, K. (2016). SqueezeNet: AlexNet-level accuracy with 50x fewer parameters and< 0.5 MB model size. *ArXiv preprint arXiv*, 1602.07360.
27. Ullah, A., Elahi, H., Sun, Z., Khatoon, A. & Ahmad, I. (2022). Comparative analysis of AlexNet, ResNet18 and SqueezeNet with diverse modification and arduous implementation. *Arabian Journal for Science and Engineering, 47*(2), 2397-2417.
28. Tuncer, T., Dogan, S. & Ozyurt, F. (2020). An automated residual exemplar local binary pattern and iterative ReliefF based COVID-19 detection method using chest X-ray image. *Chemometrics and Intelligent Laboratory Systems, 203*, 104054.
29. Khalifa, N.E.M., Taha, M.H.N., Hassanien, A.E. & Elghamrawy, S. (2022). Detection of coronavirus (COVID-19) associated pneumonia based on generative adversarial networks and a fine-tuned deep transfer learning model using chest X-ray dataset. *International Conference on Advanced Intelligent Systems and Informatics*, 234-247). Springer.
30. Alshmrani, G.M.M., Ni, Q., Jiang, R., Pervaiz, H. & Elshennawy, N.M. (2023). A deep learning architecture for multi-class lung diseases classification using chest X-ray (CXR) images. *Alexandria Engineering Journal, 64*, 923-935.
31. Li, Z., Xing, Q., Zhao, J., Miao, Y., Zhang, K. & Feng, G. (2023). COVID19-ResCapsNet: A novel residual capsule network for COVID-19 detection from chest X-ray scans images. *IEEE Access, 11*, 52923-52937.
32. Ali, M.M., Ranjan, V., Farid, A. & Raj, M. (2023). Deep learning-based Covid and pneumonia classification. *2023 Second International Conference On Smart Technologies For Smart Nation (SmartTechCon)*, 1462-1466. IEEE.
33. Kumar, S., Shastri, S., Mahajan, S., Singh, K., Gupta, S., Rani, R., Mohan, N. & Mansotra, V. (2022). LiteCovidNet: A lightweight deep neural network model for detection of COVID-19 using X-ray images. *International Journal of Imaging Systems and Technology, 32*(5), 1464-1480.
34. Shastri, S., Kansal, I., Kumar, S., Singh, K., Popli, R. & Mansotra, V. (2022). CheXImageNet: a novel architecture for accurate classification of Covid-19 with chest x-ray digital images using deep convolutional neural networks. *Health and Technology, 12*(1), 193-204.
35. Marques, G., Agarwal, D. & De la Torre Díez, I. (2020). Automated medical diagnosis of COVID-19 through EfficientNet convolutional neural network. *Applied Soft Computing, 96*, 106691.

36. Ebenezer, A.S., Kanmani, S.D., Sivakumar, M. & Priya, S.J. (2022). Effect of image transformation on EfficientNet model for COVID-19 CT image classification. *Materials Today: Proceedings, 51*, 2512-2519.
37. Sharma, P. & Sharma, V. (2024). Classification of COVID-19 utilizing CT scan images employing the EfficientNet model. *2024 International Conference on Advances in Computing Research on Science Engineering and Technology (ACROSET)*, 1-7. IEEE.
38. Ucar, F. & Korkmaz, D. (2020). COVIDiagnosis-Net: Deep bayes-SqueezeNet based diagnosis of the coronavirus disease 2019 (COVID-19) from X-ray images. *Medical Hypotheses, 140*, 109761.
39. Chowdhury, M.E.H., Rahman, T., Khandakar, A., Mazhar, R., Kadir, M.A. & Mahbub, Z.B. (2020). Can AI help in screening viral and COVID-19 pneumonia?. *IEEE Access, 8*, 132665-132676.
40. Karakanis, S. & Leontidis, G. (2021). Lightweight deep learning models for detecting COVID-19 from chest X-ray images. *Computers in Biology and Medicine, 130*, 104181.
41. Singh, K., Gaur, A., Kumar, S., Shastri, S. & Mansotra, V. (2025). Deep CP-CXR: A deep learning model for classification of Covid-19 and pneumonia disease using chest X-ray images. *Annals of Data Science*, 1-24.
42. Apostolopoulos, I.D. & Mpesiana, T.A. (2020). Covid-19: automatic detection from x-ray images utilizing transfer learning with convolutional neural networks. *Physical and Engineering Sciences in Medicine, 43*, 635-640.
43. Aljuaid, H., Adlan, H., Alkebsi, B., Alfurhood, B.S., Liotta, A. & Cavallaro, L. (2026). An experimental comparison of deep learning models for pneumonia classification from chest X-ray images. *Biomedical Signal Processing and Control, 112*, 108742.
44. Randieri, C., Perrotta, A., Puglisi, A., Grazia Bocci, M. & Napoli, C. (2025). CNN-based framework for classifying COVID-19, pneumonia, and normal chest X-rays. *Big Data and Cognitive Computing, 9*(7), 186.